Earth and Planetary Science Letters 337–338 (2012) 211–223

Contents lists available at SciVerse ScienceDirect

Earth and Planetary Science Letters

journal homepage: www.elsevier.com/locate/epsl

Letters

Hafnium isotope evidence from Archean granitic rocks for deep-mantle origin of continental crust

Martin Guitreau [a], Janne Blichert-Toft [a,*], Hervé Martin [b], Stephen J. Mojzsis [a,c], Francis Albarède [a]

[a] Laboratoire de Géologie de Lyon, Ecole Normale Supérieure de Lyon and Université Claude Bernard Lyon 1, CNRS UMR 5276, 46 Allée d'Italie, 69007 Lyon, France
[b] Laboratoire Magmas et Volcans, Université Blaise Pascal, CNRS UMR 6524, 5 Rue Kessler, 63038 Clermont-Ferrand, France
[c] Department of Geological Sciences, University of Colorado, 2200 Colorado Avenue, Boulder, Colorado 80309-0399, USA

ARTICLE INFO

Article history:
Received 28 February 2012
Received in revised form
17 May 2012
Accepted 23 May 2012
Editor: B. Marty
Available online 23 June 2012

Keywords:
TTG
zircon
Hf isotopes
continental crust
Archean
oceanic plateaus

ABSTRACT

Combined whole-rock and zircon MC-ICP-MS Lu–Hf isotope data are reported for a large collection of Archean granitoids belonging to typical tonalite–trondhjemite–granodiorite (TTG) suites. Our data demonstrate that the time-integrated Lu/Hf of the mantle source of TTGs has not significantly changed over the last 4 Gy. Continents therefore most likely grew from nearly primordial unfractionated material extracted from the deep mantle via rising plumes that left a depleted melt residue in the upper mantle. The deep mantle could retain its primitive relative element abundances over time because sinking plates are largely stripped barren of their oceanic and continental crust components at subduction zones; this process results in only small proportions (< 15–25%) of present-day continental mass getting recycled to great depths. Zircon populations extracted from the analyzed TTGs have Hf isotopic compositions broadly consistent with those of their host whole-rocks, whereas the U–Pb system in the same grains is often disturbed, causing a discrepancy that creates spurious initial ε_{Hf} values. This problem is endemic to the Archean detrital zircon record and consistent with experimental results bearing on the relative retentivity of Hf vs. U and Pb in zircon. We argue that this behavior biases the Archean zircon record toward negative ε_{Hf} values, which are at odds with the present TTG data set. If Hadean Jack Hills zircons are considered in light of these results, the mantle source of continents has remained unchanged for the last 4.3 Gy.

1. Introduction

The principle that growth of continents depletes the upper mantle of its most fertile fraction goes back several decades (Hoffman, 1988; Jacobsen and Wasserburg, 1979). A widely held tenet is that continental crust grows either by melting of the oceanic crust (Drummond and Defant, 1990; Martin, 1993) or by fluxing the mantle wedge above subduction zones (Kelemen, 1995). An alternative view holds that continents form through magmatic processing at subduction zones, not of regular oceanic crust, but of oceanic plateaus (Abouchami et al., 1990; Boher et al., 1992; Hawkesworth et al., 2010; Stein and Goldstein, 1996), which would account for the apparent episodic character of crustal growth (Albarède, 1998a; Patchett et al., 1981). Hafnium isotopes in zircons have become a widely used tracer of crustal evolution. Zircon is a ubiquitous accessory phase in all granitic rocks. It resists weathering extremely well and, hence, detrital zircons are abundant in river bedload and sands. In addition, the very low Lu/Hf of zircons allows for accurate determination of $^{176}Hf/^{177}Hf$ at the time of zircon crystallization. The advent of laser-ablation Lu–Hf isotope analysis of igneous and detrital zircons has triggered a surge in voluminous data sets with major implications for the understanding of crustal growth (Condie et al., 2009a). Yet, because of the relative scarcity of samples older than 3.4 Ga and ongoing debates over the integrity of the chronological information carried by old zircons, the ancient Hf isotope record appears less reliable than that of younger samples. This has introduced an uncomfortable degree of uncertainty into interpretations of Earth's earliest history based on Hf isotopes. Better insights into the geodynamical nature of the Hadean and early Archean eons are crucial in this regard because these times follow the demise of the postulated terrestrial magma ocean, and arguably witnessed the onset of plate tectonics.

The $\geq$4.1 Ga detrital zircons from Jack Hills, Western Australia, have attracted considerable attention because they are the sole repositories so far of direct information about the Hadean crust. Their host granites have been suggested to represent the remelting of a ca. 4.35 Ga protocrust, which carried the geochemical fingerprint of the latest residual liquids of the magma ocean, dubbed as KREEP-like by analogy with the lunar magmatic

* Corresponding author. Tel.: +33 4 72 72 84 88.
E-mail address: jblicher@ens-lyon.fr (J. Blichert-Toft).

0012-821X/$ - see front matter © 2012 Elsevier B.V. All rights reserved.
http://dx.doi.org/10.1016/j.epsl.2012.05.029

component enriched in K, rare-earth elements, and P (Blichert-Toft and Albarède, 2008; Kemp et al., 2010). It was further proposed that a connection exists between this protocrust and the source of the oldest TTGs (tonalite-trondhjemite-granodiorite) as both show indications of a mantle strongly enriched in incompatible elements (Blichert-Toft and Albarède, 2008). In order to further explore the potential relation between TTGs and the earliest Hadean/Archean crust, we report here Lu–Hf isotopic data for 2.5–4.0 Ga TTGs from a large number of localities worldwide, including most known cratons (Antarctica, Australia, Brazil, Canada, China, Greenland, India, Russia, Scandinavia, Siberia, South Africa, and Swaziland). In order to assess potential inheritance issues, Lu–Hf and Pb–Pb isotope data for individual zircons from about half of the analyzed TTG samples also are provided. The complete data set and the details of the analytical techniques (solution and laser-ablation MC-ICP-MS for whole-rocks and single zircons) together with sample descriptions are given in the following sections and the online Supplementary Material.

2. Samples

The analyzed sample suite reported herein comprises 141 TTG rocks of worldwide distribution (see Table 1 in the Supplementary Material) ranging in age from 2.5 to 4.0 Ga. The samples were either donated by colleagues during the course of this study or collected in the field by the authors. The Archean terranes represented by the samples are Enderby Land (the Napier Complex, Antarctica), the Pilbara and Yilgarn Cratons (Western Australia), the North Atlantic Craton (the Itsaq Gneiss Complex), the Slave Craton (the Acasta Gneiss Complex, Northwest Territories in Canada), the Superior Province (gneisses of the Nuvvuagittuq supracrustal belt, Québec, Canada), the Indian Craton (Dharwar, Bastar), the Kaapvaal Craton in southern Africa (Barberton, Ancient Gneiss Complex), the Baltic Shield (Finland, Norway, and Russia), the Tungus-Anabar Shield (the Sharyzhalgay uplift, central Siberia), the North China Craton (Anshan), and the São Francisco Craton (Sete Voltas, Brazil). The petrology, mineralogy, and major and trace element compositions of most of the samples, as well as their isotope compositions (notably Sr and Nd), are well documented in the literature. A description of the samples collected by the authors is given in the Supplementary Material.

3. Analytical techniques

Whole-rock sample splits used for isotope analysis were crushed and powdered in agate mortars. Zircons, if not previously separated and accompanying the whole-rock samples, were extracted using standard heavy liquid techniques and a Frantz isodynamic magnetic separator.

3.1. TTG whole-rock Lu–Hf isotope analysis by solution MC-ICP-MS

After dissolution in Parr bombs, Lu and Hf were separated from ~250 mg aliquots of whole-rock powder by ion-exchange column chromatography (at the Ecole Normale Supérieure clean laboratory in Lyon, France) and measured for their isotopic compositions by MC-ICP-MS (Nu Plasma HR) according to procedures described elsewhere (Blichert-Toft, 2001; Blichert-Toft et al., 2002, 1997; Blichert-Toft and Puchtel, 2010). Lutetium and Hf concentrations were determined by isotope dilution using a >98% pure mixed ^{176}Lu–^{180}Hf spike. The JMC-475 Hf standard was analyzed in alternation with the TTG samples and the mass fractionation-corrected ^{176}Hf/^{177}Hf ratio gave 0.282164 ± 0.000015 (2σ; $n=145$) over the 2-yr period during which these data were collected. Since this value is identical within errors to the accepted value for the JMC-475 Hf standard of 0.282163 ± 0.000009 (Blichert-Toft et al., 1997), no correction was applied to the data. Total procedural blanks for Hf and Lu were <20 pg.

The ages used to calculate the initial Hf isotopic compositions of the TTGs are the oldest concordant and reproducible ages obtained on single zircons with the Pb–Pb and U–Pb chronometers. Some of these ages were determined in this study by solution and/or laser-ablation MC-ICP-MS (see below), while others are from the literature or, in rare cases, personal communications based on unpublished data. All ages were measured on zircons that were taken either from the exact same samples as analyzed here, or from different samples from the same outcrop.

3.2. Zircon Lu–Hf and Pb–Pb isotope analyses by, respectively, solution MC-ICP-MS and ICP-MS

The TTG samples were ground to sand-sized grains and sieved to collect mineral fractions between 300 and 80 μm. The zircons were separated from these fractions using a Frantz isodynamic magnetic separator and heavy liquids. Single zircons were subsequently handpicked under a binocular microscope and abraded in an air abrasion device similar to that of Krogh (1982) to eliminate outer rims that may be either recrystallized material or represent younger overgrowths. Because severely metamict grains are particularly fragile, they tend to break or be entirely abraded away in this procedure and hence are eliminated by abrasion. Selection of individual zircons under optical microscopy favored the clearest grains without visible inclusions. Pressure and abrasion times were calibrated experimentally and were critical parameters because of the fragile nature of old, potentially metamict zircons. Cathodo-luminescence (CL) images of most of the TTG zircon populations were acquired on a JEOL JSM-5910LV in Clermont-Ferrand and used to identify structural heterogeneities, as well as to estimate average potential overgrowth widths in order to abrade the zircons to recover only their cores. Because the zircon grains were always covered by metal dust after the abrasion procedure, and because (younger) outgrowths may not have been entirely removed in the process, the zircons were further leached prior to dissolution. We deliberately used short leaching times with concentrated acids (see details below) as opposed to the standard procedures described by Corfu (2000) and Das and Davis (2010), which call for long durations with weak acids. This is because Hadean and Archean zircons are old enough to have been massively exposed to the alpha-decay of U-series isotopes and, hence, readily dissolve in acid at room pressure and temperature due to their often metamict condition. The use, therefore, of a short-duration bath of strong acid results in well-leached grain surfaces, which is where the potential contamination resides. This approach to eliminate younger, more resistant, external margins does not result in dissolution of partly amorphized cores. The use of more dilute acids for longer durations of time, by contrast, potentially results in the preferential dissolution of the most damaged parts of the zircons, such as the oldest igneous core regions. This procedure could, therefore, destroy the principal parts of the zircons, which are the most important for studies such as the present one, while preserving younger, more resistant domains such as overgrowths or other less damaged parts that include the unwanted material. The abundant cracks typical of ancient metamict zircons and their old igneous cores represent a ready conduit for weak acids at long exposure times. To avoid this problem, our three-step leaching procedure consists of successive baths of concentrated double-distilled HF (a few minutes at room temperature),

concentrated distilled HNO_3 (a few minutes at room temperature), and 6 N distilled HCl (10 min at 135 °C). Subsequently, individual abraded and leached zircons were transferred into 0.5 ml Savillex® beakers to which a mixture of concentrated double-distilled HF and traces of concentrated distilled HNO_3 were added. Batches of 16 Savillex® beakers were loaded in a 4748 Parr® bomb for digestion in an oven at 240 °C for at least 24 h (Parrish, 1987). The dissolved grains were then transferred into clean Savillex® beakers, dried down, and re-dissolved in 1 ml (to be able to remove a precise aliquot volume) distilled 8 N HNO_3 on a hot plate. A 5% aliquot (50 μl) was taken for each sample for Lu/Hf ratio measurement and the HNO_3 subsequently evaporated to dryness. Lutetium and Hf concentrations were determined on the aliquot using a ThermoFinnigan Element 2 ICP-MS at the Ecole Normale Supérieure in Lyon, and the $^{176}Lu/^{177}Hf$ ratios were calculated from the measured concentrations. The 95% that remained in the beakers from the original zircon solution was dissolved in distilled 1 N HCl:0.1 N HF and loaded onto 0.18 ml Teflon cation-exchange columns (AG50W-X8, 200–400 mesh). Hafnium is in the form of a negative fluoride complex and therefore does not stick on this column and is immediately recovered. Lead is subsequently eluted with distilled 2.5 N HCl. The Pb isotope compositions were measured on the Element 2 ICP-MS and the Hf isotope compositions on the Nu Plasma HR MC-ICP-MS, both at the Ecole Normale Supérieure in Lyon.

The JMC-475 Hf standard was analyzed in alternation with the zircon samples and the mass fractionation-corrected $^{176}Hf/^{177}Hf$ ratio gave 0.282162 ± 0.000017 (2σ; $n=87$) over the 2-yr duration of sessions of single zircon data collection. Again, this value is within error bars of the accepted value for the JMC-475 Hf standard eliminating the need for normalization. Total procedural blanks were <10 pg for Lu and <20 pg each for Hf and Pb. The relative abundance of oxides was $<2\%$, which represents a negligible correction for the present analyses. Fluctuations in the ion beams of Lu, Hf, and Pb were monitored using a 1 ppb internal In standard. The isobaric interference of ^{204}Hg on ^{204}Pb ($<0.1\%$) was corrected using ^{200}Hg and a $^{204}Hg/^{200}Hg$ ratio of 0.2974. As it was considered that ^{204}Pb is largely derived from mineral inclusions and the blank, each zircon was corrected using the modern common Pb isotope composition of Stacey and Kramers (1975). Sample-standard bracketing was done using the NIST SRM 981 standard and the values of Eisele et al. (2003). The equations used are those of Albarède et al. (2004). The Th/U ratios of the zircons were calculated using the measured $^{208}Pb/^{206}Pb$ and the age T of the zircon given by its $^{207}Pb^*/^{206}Pb^*$ ratio (*=radiogenic):

$$\frac{^{208}Pb^*}{^{206}Pb^*} = \frac{^{232}Th}{^{238}U} \times \frac{e^{\lambda_{232Th}t}-1}{e^{\lambda_{238U}t}-1} \quad (1)$$

This calculation assumes that the Th/U and the $^{208}Pb/^{206}Pb$ ratios of the zircon have not been disturbed significantly throughout its history, which we consider to be a reasonable assumption as these elements are relatively immobile (Cherniak et al., 1997a). Although the Th/U ratio in zircons can range from ~ 10 to 1×10^{-4}, it has been shown (e.g., Hoskin and Schaltegger, 2003) that Th/U of ~ 0.5 is a reasonable average estimate for igneous zircons, while Th/U <0.2 is more representative of metamorphic zircons. The majority of the zircons analyzed in this study have Th/U ratios consistent with a magmatic origin. The ^{207}Pb–^{206}Pb ages were calculated by iterative convergence using the Excel® goal-seek function.

3.3. Zircon Lu–Hf and U–Pb isotope analyses by, respectively, laser-ablation MC-ICP-MS and ICP-MS

The zircons analyzed by laser-ablation MC-ICP-MS were hand-picked under a binocular microscope, placed on double-sticky tape, and mounted in epoxy. The 2.54 cm epoxy mounts were first polished on 5 μm silicon-carbide mats and then with 0.5 μm diamond paste and distilled water. Prior to laser ablation analysis, the zircons were imaged by CL using either a Leo Supra 35VP scanning electron microprobe (SEM) at the University of Idaho (Moscow), or a JEOL JSM6510 SEM at the Centre de Recherches Pétrographiques et Géochimiques in Nancy (France). The acquired CL images were used to assess the internal structure of the zircons in order to target their cores and areas where the best-preserved parts with magmatic zoning were still visible. U–Pb analyses were carried out using a 213 nm New Wave Research Nd-YAG laser connected to a ThermoFinnigan Element 2 (LA-ICP-MS). Hafnium isotope measurements were performed using the same laser but connected to a ThermoFinnigan Neptune (LA-MC-ICP-MS). All laser ablation Hf and Pb isotope work was carried out at the Department of Geology of Washington State University, Pullman. The ablation cell for both types of measurements was filled with He. The carrier gas used in both instruments was Ar, but N_2 was added to increase the Hf ion beam intensity. For the U–Pb isotope analyses, the laser spot size was 30 μm using a frequency of 5 Hz in order to avoid saturation of the collectors due to the high radiogenic Pb abundances in Archean zircons. For particularly U-rich grains, the frequency was reduced to 3 Hz. For the Hf isotope analyses, laser spot sizes of 40 μm at 10 Hz were used. U–Pb corrections were made by sample-standard bracketing using both Peixe (Dickinson and Gehrels, 2003) and FC-1 (Paces and Miller, 1993) zircon standards. Isobaric interferences of ^{204}Hg on ^{204}Pb were corrected using ^{202}Hg and a $^{204}Hg/^{202}Hg$ ratio of 0.2301 to determine $^{204}Pb/^{206}Pb$ ratios that were always below 0.001. For the Hf isotope measurements on the Neptune, mass bias, isobaric interferences (Yb and Lu on mass 176), and instrument drift were corrected according to the procedures described by Bahlburg et al. (2011) and Gaschnig et al. (2011). The precision on $\varepsilon_{Hf}(T_0)$ can be assessed by examination of the 2-σ intervals of the 396 in-situ measurements undertaken here (Fig. 1). The analyses form a consistent histogram (Fig. 1) with no objective justification for ignoring (i.e., discarding) specific measurements

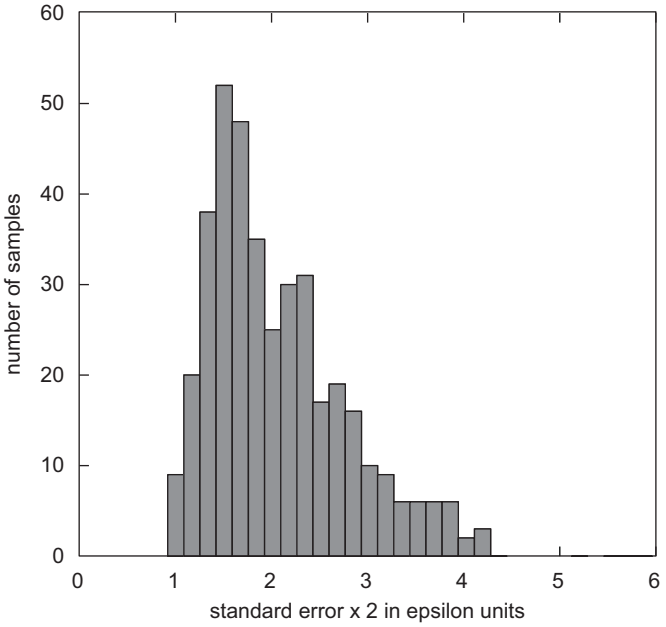

Fig. 1. Histogram of 2-σ error bars for in-situ Hf isotope measurements of single zircons in epsilon units. This plot shows that the data set is of consistent quality: for a single population of points with a similar number of measurements, the variances are expected to follow a chi-squared distribution. About 90 percent of the samples have 2-σ errors <3 epsilon units.

and with a range that is consistent, given the large number of data, with that obtained in previous investigations on the same instrument.

3.4. The zircon Hf isotope database

A zircon Hf isotope database was compiled for this study in order to provide a broader context within which the TTG data are discussed. It comprises 12,786 data points, with the vast majority of the data (91%) being derived from detrital zircons (11,698). The references that this compilation is based on are listed in the Supplementary Material. Zircons with a U–Pb discordance in excess of 5% and with Th/U ratios >1 and <0.15, as calculated from their $^{208}Pb^*/^{206}Pb^*$ and ages, were disregarded. The initial ε_{Hf} values of literature samples were calculated using the CHUR values of Bouvier et al. (2008) ($^{176}Hf/^{177}Hf=0.282785$ and $^{176}Lu/^{177}Hf=0.0336$) and the ^{176}Lu decay constant of 1.867×10^{-11} of Söderlund et al. (2004), identical to the original determination by Scherer et al. (2001) but with reduced error bars.

4. Results

4.1. TTG whole-rock and single zircon Lu–Hf isotope data

The initial $\varepsilon_{Hf}(T_0)$ of the 141 TTG whole-rock samples analyzed here (Table 1, Supplementary Material) are shown in Fig. 2 on the background of zircon data from both the literature (12,786 zircons) and the present study (340 zircons analyzed by wet chemistry and in-situ techniques filtered from 615 zircons from 72 of the 141 TTGs; Tables 2–6, Supplementary Material). As pointed out by Zeh et al. (2007), igneous zircons extracted from the same sample often show a positive correlation between their measured (i.e., apparent) $^{207}Pb/^{206}Pb$ ages T_0 and $\varepsilon_{Hf}(T_0)$, indicating that zircons with strongly negative $\varepsilon_{Hf}(T_0)$ have experienced severe Pb loss, while their Hf isotopes have remained unaffected. Lenting et al. (2010) demonstrated experimentally that these different conducts of the U-Pb and Lu-Hf isotope systems are a general feature of zircons under metamorphic conditions. This means that for these zircons, their initial Hf isotopic compositions are calculated at the wrong age and result in incorrect initial ε_{Hf} values. This conclusion applies to a substantial fraction of the single zircons in Fig. 3. We therefore regard all samples for which $\varepsilon_{Hf}(T_0)$ correlates with age as suspect. This is the reason why discordant zircons (for LA-ICP-MS and ion microprobe analyses) and zircons with distinctly non-magmatic Th/U ratios (for solution MC-ICP-MS analyses) have been filtered out in Fig. 2. Fig. 4 shows that, after filtering, 10% of the zircons from the laser-ablation data set and 18% of the zircons from the solution data set fall outside a band of ±5 epsilon units about the 1:1 correlation line, with 75% and 61% of the data, respectively, falling within a ±2 epsilon unit band about this line. Given the substantial scatter of $\varepsilon_{Hf}(T_0)$ observed in Fig. 2 at a given age, we consider that the $\varepsilon_{Hf}(T_0)$ in the zircons and their host TTG whole-rocks analyzed in this work are reasonably consistent. This indicates that the assumed TTG ages are correct and that the TTG Lu–Hf isotope systematics have not been significantly disturbed subsequent to TTG magma crystallization. Fig. 4 also demonstrates that the inheritance of older zircons plays a negligible role and that laser-ablation and solution chemistry zircon isotope data are mutually consistent. This last observation is further strengthened by the results shown in Fig. 5, which displays the similar $^{176}Hf/^{177}Hf$ ratios obtained on zircons that were first analyzed by laser-ablation, then dismounted, dissolved, and measured by solution MC-ICP-MS. Additionally, Fig. 5 illustrates that both present-day and initial Hf isotope compositions agree between the two techniques, whereas Pb–Pb ages and $^{176}Lu/^{177}Hf$ often disagree to variable degrees.

Given the large size of the database (12,786 samples), a 2-dimensional histogram presentation has been chosen for Fig. 2 because it allows the main data structure to stand out and minimizes the spread caused by outliers. The present Hf isotope data corroborate the observation that suprachondritic $\varepsilon_{Hf}(T_0)$ values existed prior to 2.9 Ga (Hoffmann et al., 2011; Vervoort and Blichert-Toft, 1999). The Archean TTG whole-rock data in this study tend to populate the low-density domains of $\varepsilon_{Hf}(T_0)>0$, with the exception of samples older than 3.8 Ga. These data are, therefore, consistent with the $\varepsilon_{Nd}(T_0)>0$ commonly reported for these rocks (Hoffmann et al., 2011; Vervoort and Blichert-Toft, 1999), and attests to overall congruent Hf–Nd isotope behavior. Moderately radiogenic Nd and Hf is a common feature of Archean and early Proterozoic mantle-derived magmas

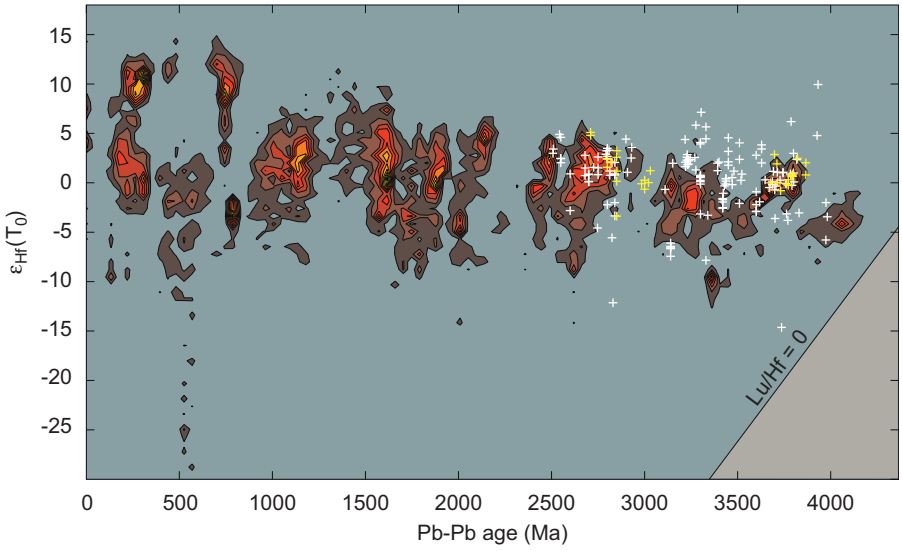

Fig. 2. Two-dimensional histogram of initial $\varepsilon_{Hf}(T_0)$ of detrital and magmatic zircons as a function of their Pb–Pb age. Contours correspond to 10% intervals (deciles). Only data from zircons with less than 5% discordance, and with Th/U ratios between 0.15 and 1.0 and consistent with $^{208}Pb/^{206}Pb$ ratios, have been included in the compilation. TTG whole-rock data are superimposed as white (this study) and yellow (Hoffmann et al., 2011) crosses. The gray triangle in the lower right-hand corner shows the forbidden zone with $Lu/Hf\leq0$. (For interpretation of the references to color in this figure legend, the reader is referred to the web version of this article.)

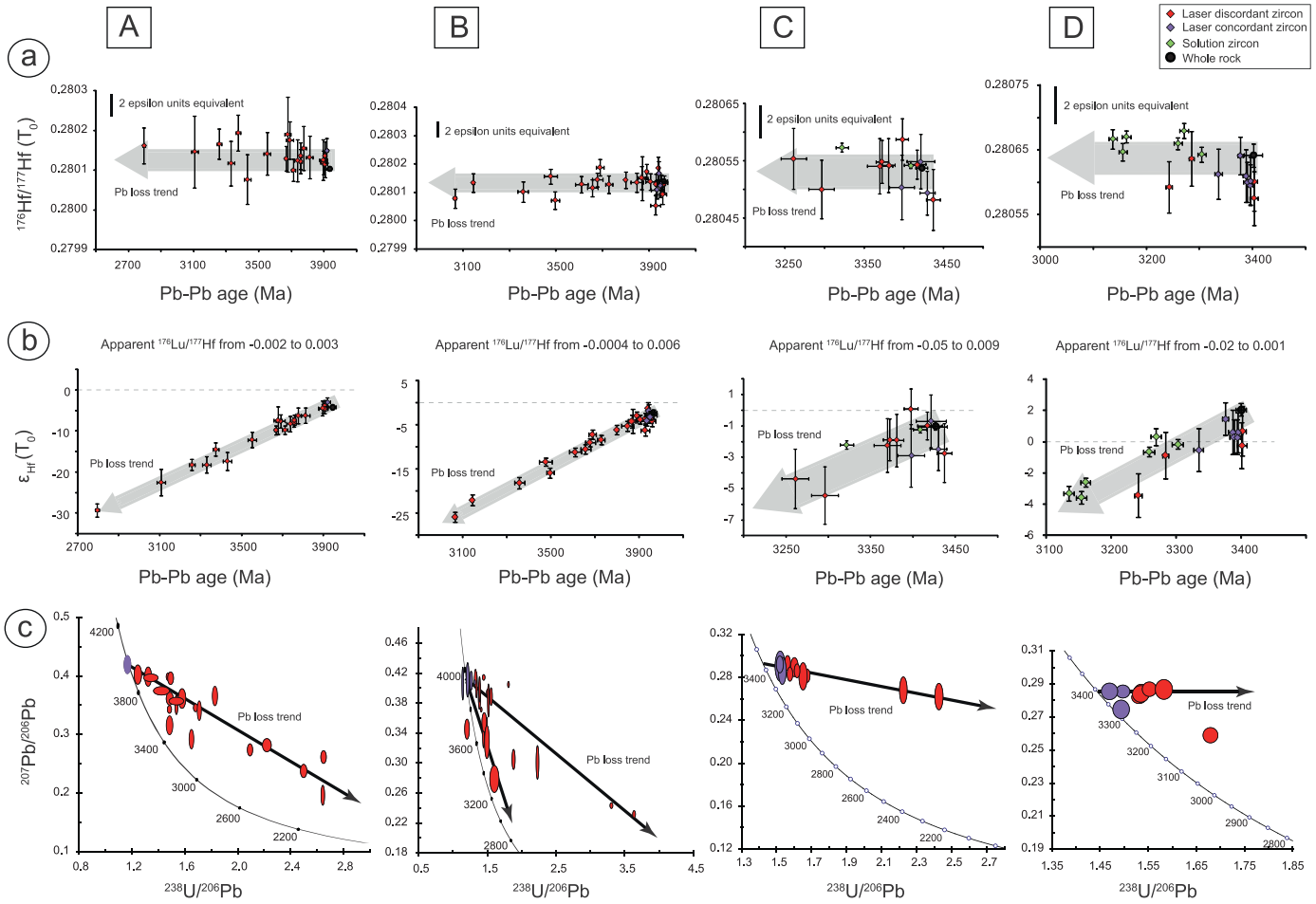

Fig. 3. $^{176}Hf/^{177}Hf$ (T_0) and ε_{Hf} (T_0) versus Pb–Pb age diagrams combined with Tera–Wasserburg ($^{207}Pb/^{206}Pb$ versus $^{238}U/^{206}Pb$) concordia plots for zircon populations from four representative TTG samples. Panels A, B, C, and D refer to, respectively, samples AG09-008gt (Acasta gneiss, Slave Craton, Canada), AG09-016 (Acasta gneiss, Slave Craton, Canada), SV11 (Sete Voltas, São Francisco Craton, Brazil), and 40-03 (Onot terrane, Tungus-Anabar shield, Siberia). Diagrams (a) illustrate that, among a given TTG zircon population, $^{176}Hf/^{177}Hf$ (T_0) is generally consistent within the quoted error bars, whereas $^{207}Pb/^{206}Pb$ ages vary well beyond analytical uncertainties for discordant grains (red diamonds). In contrast, concordant grains (purple diamonds) have consistent $^{176}Hf/^{177}Hf$ (T_0) and $^{207}Pb/^{206}Pb$ ages. Note that in panels C and D, single zircons analyzed by solution chemistry (green diamonds) show similar behavior as zircons analyzed by laser-ablation. The sample displayed in panels D further shows that the solution zircon population has slightly more radiogenic Hf than the in-situ zircon population resulting in a shift of about one epsilon unit. This is due, likely, to slight overcorrection of the large ^{176}Yb and ^{176}Lu isobaric interferences for the laser-ablation analyzed zircons, whereas the zircons analyzed by solution chemistry and, therefore, free of any isobaric interferences due to efficient purification of Hf by ion-exchange chromatography, give more reproducible $^{176}Hf/^{177}Hf$ (T_0). Despite the complex metamorphic histories of TTGs, it appears that single zircons of these rocks analyzed by solution chemistry yield the same results as zircons analyzed by laser-ablation, indicating that either the zircon populations are simple, or the combined air-abrasion and leaching techniques undertaken in the present study were efficient enough to preserve only the igneous cores of the zircons. Note also that $^{176}Hf/^{177}Hf$ (T_0) of the TTG whole-rocks (black circles) are consistent with $^{176}Hf/^{177}Hf$ (T_0) of the zircon populations. Diagrams (b) show the effect of perturbed (or discordant) ages (i.e., different from the crystallization age) on the ε_{Hf} (T_0) of the zircon populations. Because of the very low $^{176}Lu/^{177}Hf$ ratio ($\sim$0.0005) of zircons (Fig. 9), their $^{176}Hf/^{177}Hf$ (T) is virtually insensitive to age corrections, while this is not true for ε_{Hf} (T). Slopes regressed with Isoplot® indicate apparent $^{176}Lu/^{177}Hf$ ratios of $\sim$0, which is incompatible with radiogenic ingrowth in any geological reservoir but zircons. Note that these trends are particularly well defined for the zircons in panels A-(b) and B-(b) compared to those in panels C-(b) and D-(b) because of a larger overall spread in $^{207}Pb/^{206}Pb$ ages for the former two samples. It appears that concordant zircons give reproducible ε_{Hf} (T_0) and $^{207}Pb/^{206}Pb$ ages within error bars. Diagrams (c) are Tera–Wasserburg concordia plots that demonstrate that it is disturbance of the U–Pb isotopic system (Pb loss) which is responsible for the age variability. (For interpretation of the references to color in this figure legend, the reader is referred to the web version of this article.)

(Bennett et al., 1993; Shirey and Hanson, 1986; Vervoort and Blichert-Toft, 1999). Even when potentially contaminated or peripheral samples are filtered out (Albarède and Brouxel, 1987; Stein and Hofmann, 1994) the apparent Sm/Nd of the mantle source inferred from the ε_{Nd} (T_0) evolution curve is, as demonstrated by DePaolo (1980), definitely smaller than that of the upper mantle (e.g., Workman and Hart, 2005). In this context, we suggest that the apparently uncommon radiogenic Hf among $>$4.0 Ga old zircons in Fig. 2 is largely statistical in nature: both positive and near-chondritic ε_{Hf} (T_0) values have been reported for Jack Hills zircons (Blichert-Toft and Albarède, 2008; Harrison et al., 2005), even for homogeneous grains. Parametric Student and non-parametric Wilcoxon tests based on initial $^{176}Hf/^{177}Hf$ ratios show that the data set of Harrison et al. (2005) is indistinguishable from that of Blichert-Toft and Albarède (2008) and Kemp et al. (2010) (Fig. 6). However, when considering the initial ε_{Hf} values, the data set of Kemp et al. (2010) and the most recent data set of Harrison et al. (2008) become statistically distinct from that of Blichert-Toft and Albarède (2008) and Harrison et al. (2005) because the former two do not include values above a certain negative ε_{Hf} (T_0) threshold (Fig. 7). We therefore emphasize that, even if it is a rare signal, radiogenic Hf (i.e., positive ε_{Hf} (T_0)) existed at the time the source rock of the Jack Hills zircon host rock crystallized. The smaller frequency of $>$4.0 Ga old zircons with radiogenic Hf may be the result of undersampling simply because the Jack Hills outcrop does not reflect the wide watersheds that supplied the detrital zircons used for other studies. Likewise, $>$3.9 Ga Acasta samples occur as

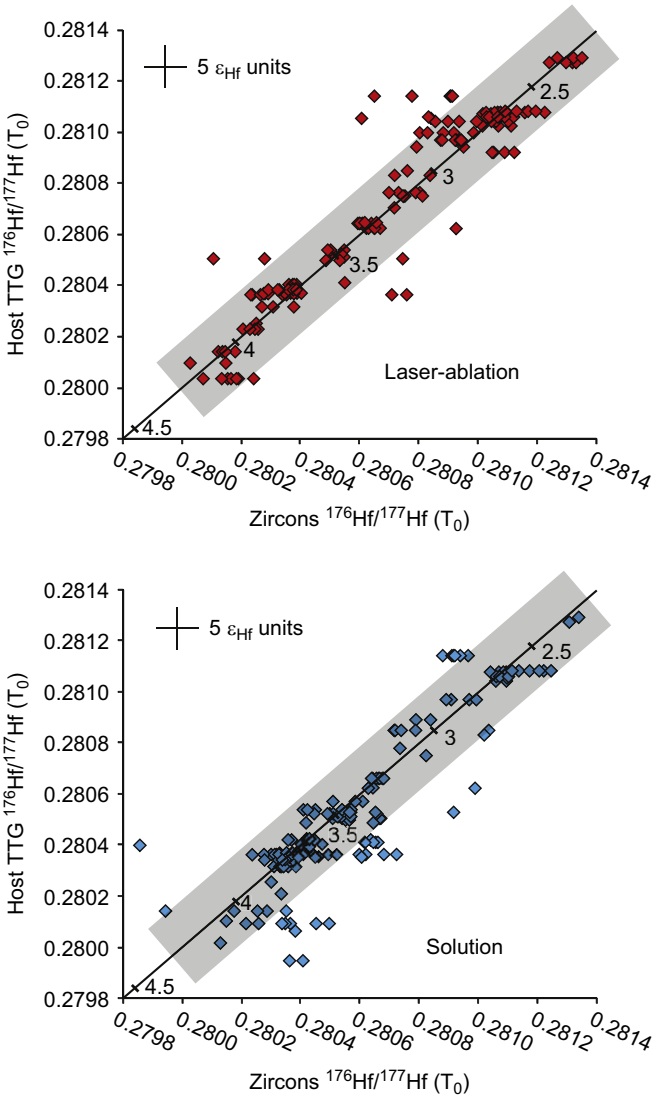

Fig. 4. Correspondence of $^{176}Hf/^{177}Hf$ (T_0) between individual zircons analyzed by solution (bottom) and laser-ablation (top) MC-ICP-MS and their host TTG whole-rocks (analyzed by solution MC-ICP-MS). Only concordant zircons (laser ablation) and zircons with Th/U ratios (solution) in the range of 0.15–1.0 have been considered. The tick marks and numbers on the 1:1 line refer to the CHUR model ages (Ga). The shaded band about the 1:1 correlation line represents ± 5 epsilon units. The general consistency of the two types of data indicates mutual agreement between solution chemistry and laser-ablation techniques. The overall distribution of the data along the 1:1 trend means that inheritance of older zircons is insignificant. The horizontal spread towards more radiogenic Hf isotope compositions observed for zircons analyzed by solution chemistry is attributed to incomplete elimination of the outer parts of the grains after abrasion and leaching.

small meter-thick sheets in otherwise younger orthogneisses (Bowring et al., 1989) and may be local biased representatives of the common mid-crust at that time.

4.2. Impact on the results from the choice of reference frame for the Lu–Hf isotope system

The modern chondritic Lu–Hf reference may be perceived as an issue but, beyond the confusion introduced by multiple normalization values, the choice of one over the other is inconsequential as the two reference frames currently in use are nearly identical within the quoted error bars. For example, adopting the 2008 chondritic parameters (Bouvier et al., 2008) instead of the 1997 reference (Blichert-Toft and Albarède, 1997) changes the epsilon values from +0.45 for modern samples to −0.36 at 3 Ga, which is within the analytical errors of both the samples and the reference parameters themselves.

4.3. Comparison between laser-ablation and single grain dissolution techniques

Forty-one carefully selected zircons were analyzed by laser-ablation and then extracted from their mounts to be dissolved separately according to the single grain dissolution technique described earlier (Table 6, Supplementary Material). The zircons were chosen based on CL imagery, concordant ages, small $^{176}Hf/^{177}Hf$ error bars, and reproducible age and/or similar $^{176}Hf/^{177}Hf$ from different spots on the same grain. The results are presented in Fig. 5 and illustrate that $^{207}Pb/^{206}Pb$ ages (Fig. 5a) as well as $^{176}Lu/^{177}Hf$ (Fig. 5b) measured by solution and laser-ablation often do not agree. In particular, the solution Pb–Pb ages are systematically younger than the laser-ablation ages and the Lu/Hf ratios determined by laser-ablation are higher in most cases than those measured by solution. In contrast, $^{176}Hf/^{177}Hf$ is far more consistent between the two techniques, forming a positive correlation with a slope of 0.97 ± 0.07 (Fig. 5c). The same is true for initial $^{176}Hf/^{177}Hf$, which plots on a trend with a slope of 0.94 ± 0.08 (Fig. 5d). Although age and $^{176}Lu/^{177}Hf$ disagree, the latter is so low that differences in calculated initial Hf isotopic compositions due to age correction are generally insignificant. Considering metamictization processes and volume diffusion theory, these results are consistent with experiments of Cherniak et al. (1997a, 1997b) that show Hf to be a highly retentive element within the zircon lattice, whereas Pb and Lu are relatively mobile. This is consistent with the experiments of Lenting et al. (2010). By metamictization we refer to partly and localized destroyed zircon lattices, not to completely amorphized grains (Utsunomiya et al., 2004). We attribute age differences to localized Pb loss within zircon grains or their inclusions (Carson et al., 2002) (not sampled in general by laser-ablation but unavoidable by solution chemistry) and $^{176}Lu/^{177}Hf$ ratio differences to magmatic zonation within the zircons and/or perhaps Lu loss. The observed $^{176}Lu/^{177}Hf$ differences between the two techniques also could derive from Lu–Hf fractionation during acid leaching of the abraded zircon grains (Lu being a 3+ rare-earth element and Hf being a 4+ high-field-strength element), as observed for U and Pb (Mattinson, 2005). As mentioned above, however, zircon Lu/Hf ratios are so low that this disturbance is essentially inconsequential to the initial Hf isotope compositions. In summary, we consider the in-situ concordant laser-ablation ages to be the correct ages. The $^{207}Pb^*/^{206}Pb^*$ of discordant zircons, whether acquired by wet chemistry of whole grains or by laser-ablation of selected spots, may not reflect the time of zircon crystallization if they were subject to ancient Pb loss episodes.

5. Discussion

Fig. 2 reinforces evidence accumulated over half a century (Condie et al., 2009a; Gastil, 1960) that the crustal growth record is episodic. The conspicuous gap in crustal growth at 2.3–2.4 Ga identified by Condie et al. (2009a) also is evident in Fig. 2. We will now focus on the preservation of the crustal growth record, the effect of crustal reworking, and the nature of crustal growth.

5.1. Preservation of the crustal growth record

It has been proposed that age peaks represent artifacts of preservation (Gurnis and Davies, 1986; Hawkesworth et al., 2010). If so, the U–Pb age records of igneous and detrital zircons

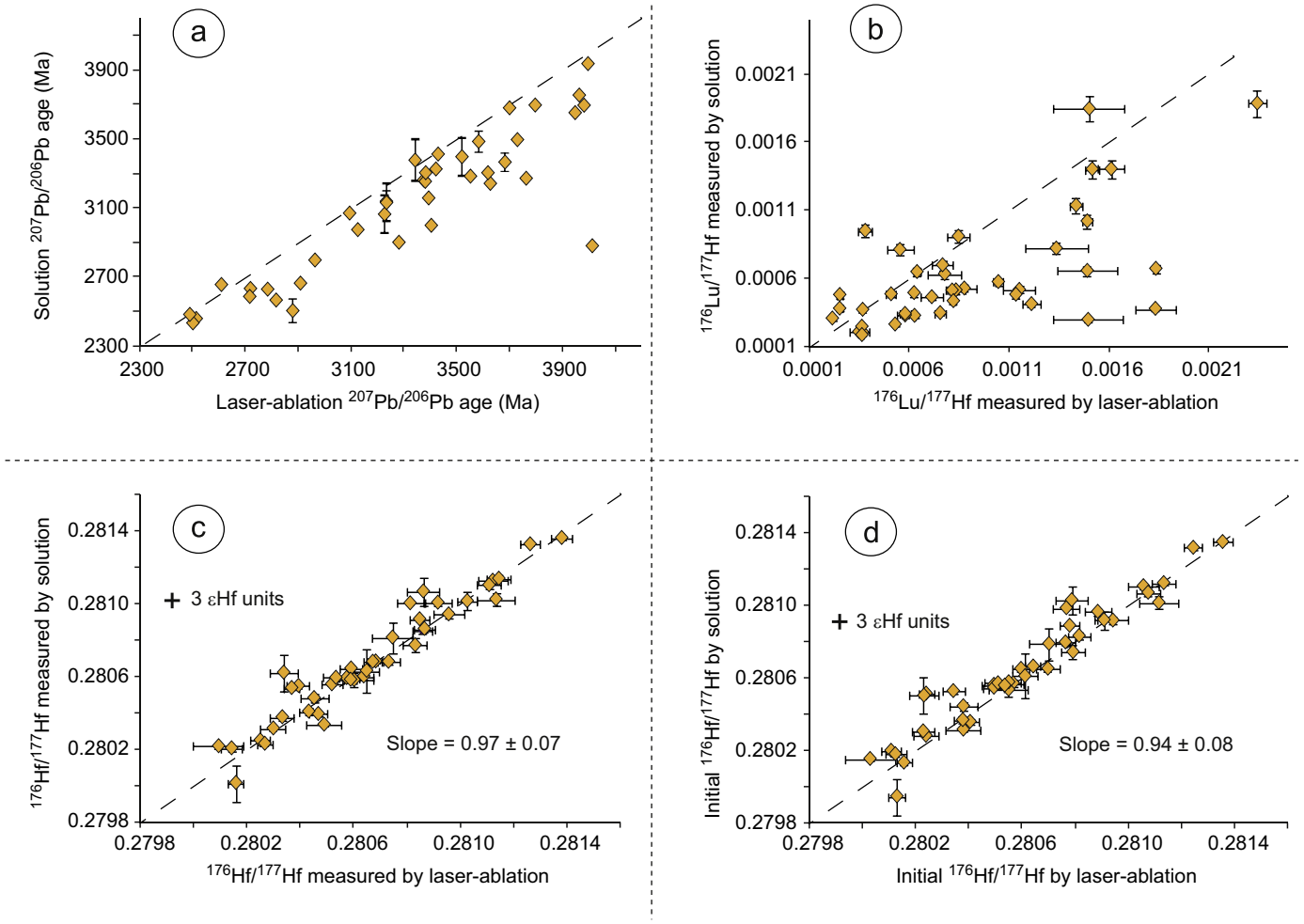

Fig. 5. Diagrams comparing zircons analyzed by both laser-ablation and bulk solution chemistry for their $^{207}Pb/^{206}Pb$ ages (a), their $^{176}Lu/^{177}Hf$ (b), their present-day $^{176}Hf/^{177}Hf$ (c), and their initial $^{176}Hf/^{177}Hf$ (d). These plots illustrate that measured $^{207}Pb/^{206}Pb$ ages and $^{176}Lu/^{177}Hf$ ratios often are significantly different between the two techniques, whereas present-day $^{176}Hf/^{177}Hf$ ratios are highly consistent within the analytical uncertainties and, hence, that isobaric interferences on mass 176 during laser-ablation are well corrected for. Initial $^{176}Hf/^{177}Hf$ ratios are also in good agreement between the laser-ablation and solution chemistry methods because the average zircon $^{176}Lu/^{177}Hf$ is so low that age correction is usually negligible even if age differences exceed the analytical uncertainty. In contrast, the consequences of the variable $^{207}Pb/^{206}Pb$ ages are severe for the ε_{Hf} determination due to the sensitivity of the CHUR reference to changes in age (the CHUR reference frame changes rapidly with age: ~2.2 ε_{Hf} units per 100 Ma). We consider $^{207}Pb^*/^{206}Pb^*$ ages of concordant zircons to represent the true zircon crystallization ages. The younger ages often obtained by wet chemistry likely reflect ancient Pb loss episodes in the zircons or their inclusions.

should mirror each other, which is precluded by available evidence (Condie et al., 2009a). Fig. 2 illustrates that, prior to 1.7 Ga, zircon ε_{Hf} (T_0) values decrease during individual orogenic cycles and, therefore, the degree of crustal reworking increased with particularly clear examples at 2.1, 2.4, and 3.8 Ga. Evidence that at the time of supercontinents young terranes are selectively removed remains unsubstantiated. In contrast, evidence shows that continental assembly efficiently accretes landmasses and oceanic plateaus (Boher et al., 1992; Schubert and Sandwell, 1989).

5.2. *Juvenile versus reworked orogenic segments.*

The impact of crustal reworking on the interpretation of the present data set must be assessed. Many orogenic belts consist of vast expanses of 'juvenile' areas, in which the contribution of pre-existing continental material to new crust is minor and crustal residence time is short. This is in particular the case of Abitibi (2.7 Ga) (Davis et al., 2005), the Birimian (2.1 Ga) of West Africa (Boher et al., 1992), and Arabia (0.6 Ma) (Stein and Goldstein, 1996). The orogenic cycle, which leads from the protolith to new stable continental crust, is invariably short (<150 Ma). In contrast, radiogenic and stable isotope geochemistry of granites show that some other orogenic segments are clearly reworked, with the 1.8 Ga terranes of the Svecofennian (Condie et al., 2009a; Hoffman, 1988; Patchett et al., 1987) being a prime example. More than three decades of geochemical work performed on recent granites have demonstrated that if crustal reworking is indeed common, its importance in a particular orogenic segment can be readily and unequivocally assessed by combining oxygen and radiogenic isotopes. An illustrative example of such disentanglement is the 90–130 Ma old Peninsular Range batholith of California (DePaolo, 1981; Kistler et al., 2003; Taylor and Silver, 1978). By restricting the analysis to the granites with oxygen isotopes close to mantle values, the least radiogenic Sr, and the most radiogenic Nd (and Hf), the 'mantle component' and 'mantle-like' granites clearly show up in the data and can be targeted for further insight into the nature and evolution of their mantle source. With the renewed interest for the understanding of crustal growth, a similar approach was successfully adopted by Kemp et al. (2007, 2006) for older granites. Here we therefore focus on the most radiogenic part of the two-dimensional histogram of Fig. 2 (the most negative ε_{Hf} (0) values clearly being the products of reworking). This strategy is supported by the lack

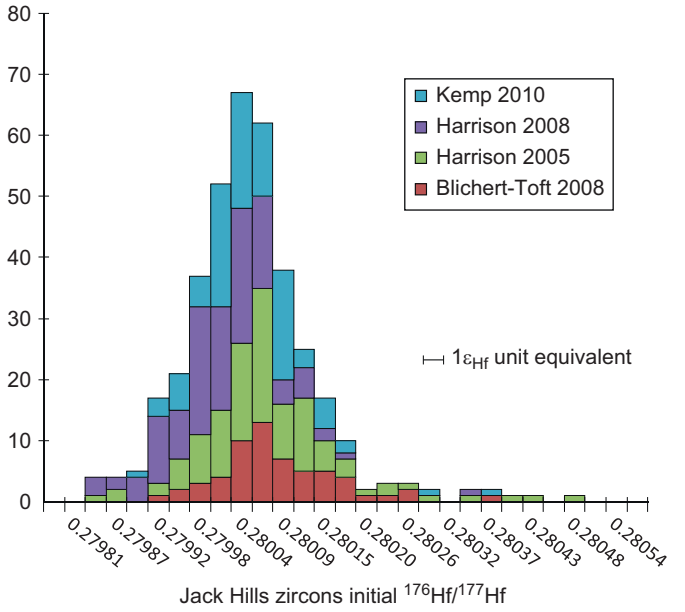

Fig. 6. Histograms of the initial $^{176}Hf/^{177}Hf$ distribution for four different Jack Hills zircon data sets (Blichert-Toft and Albarède, 2008; Harrison et al., 2005, 2008; Kemp et al., 2010). All the distributions are similar and centered around the same maxima. Each increment in initial $^{176}Hf/^{177}Hf$ is $2.8.10^{-5}$, which corresponds to 1 ε_{Hf} unit.

of strong contrast between orogens in which the bulk of the material is juvenile, such as in the Abitibi (2.7 Ga) and the Birimian (2.1 Ga), and those dominated by reworking, such as the 1.8 Ga terranes of the Svecofennian shield. The comparison of these terranes shows that assimilation of older crust does not define the first-order Hf isotopic characteristics of crustal segments. In addition, the effect of assimilation of continental crust on the apparent time-integrated Lu/Hf ratio of the mantle source is in any case minimal for most of crustal history: a given variation $\delta\varepsilon_{Hf}$ is equivalent to a relative variation of the time-integrated Lu/Hf of $\delta\varepsilon_{Hf}/21.8\times(4.5-T)$, where T is the age in Ga of the orogeny in question. Using as $\delta\varepsilon_{Hf}$ the difference between the density maxima (Fig. 2) and the mantle ε_{Hf} values at the same age from Vervoort and Blichert-Toft (1999), this effect is $\pm 20\%$ at 3.5 Ga and $\pm 10\%$ at 2.5 Ga.

5.3. *The nature of crustal growth.*

The time-integrated $^{176}Lu/^{177}Hf$ (parent–daughter) ratios of the source were calculated from the age and ε_{Hf} (T_0) of each sample using the ε_{Hf} (4.568 Ga) value of Bouvier et al. (2008). This use of apparent time-integrated Sm/Nd and Lu/Hf is essentially equivalent to the μ analysis of Pb isotope evolution, and has been used for decades in order to decipher the dynamics of planetary mantles (e.g., Nyquist and Shih, 1992). Fig. 8 shows that, when the TTG data are taken into account, the $^{176}Lu/^{177}Hf$ ratio of the mantle source of continents has not varied much (0.032–0.038 ($\pm 10\%$)) with respect to the chondritic value of 0.0336 (Bouvier et al., 2008) over the last 3.8 Gy. Again, the pre-3.8 Ga samples (notably Acasta and Jack Hills) are exceptions (Jack Hills zircons not visible in Fig. 8 because of their relative scarcity) that may attest to either undersampling of the crust from that time or some transient effects inherited from the original differentiation of the Earth. Highly radiogenic ε_{Hf} (T_0) values seem to have become common only in the late Proterozoic. The dramatic reduction in Lu/Hf variability during the first 0.7–1 Gy mirrors the possible reduction in $^{142}Nd/^{144}Nd$ variability as put forth by Bennett et al. (2007). This decrease in

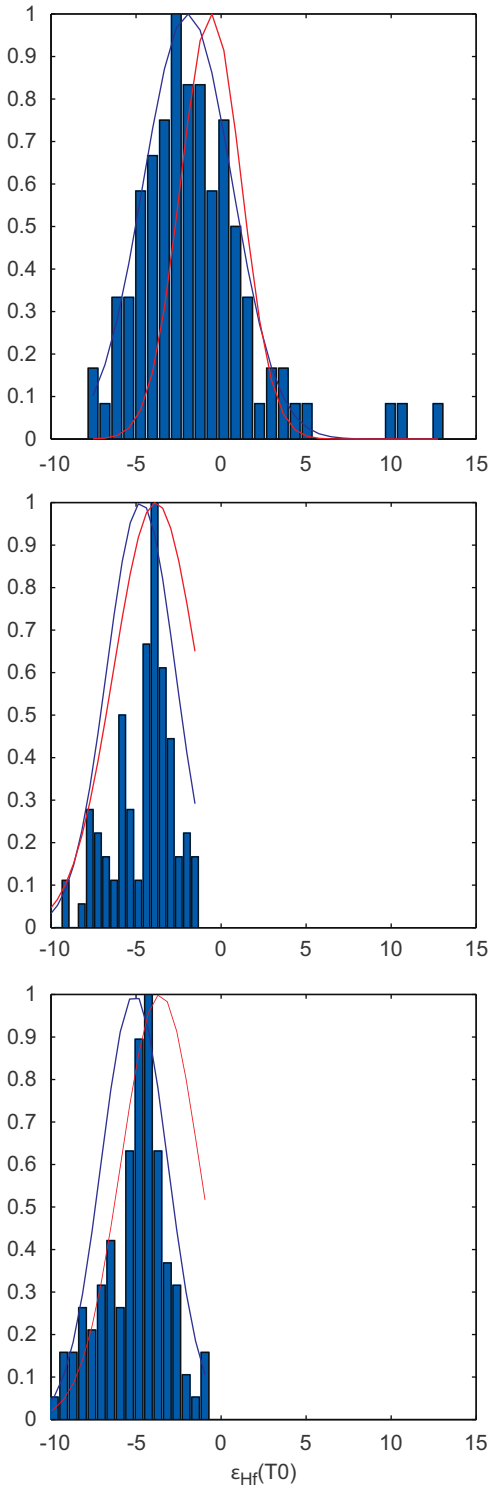

Fig. 7. Histograms of the solution-MC-ICP-MS data sets of Harrison et al. (2005) and Blichert-Toft and Albarède (2008) (top panel), and the in-situ data sets of Kemp et al. (2010) (middle panel) and Harrison et al. (2008) (bottom panel) showing that, in contrast to the solution data set, the two in-situ data sets are biased with respect to their predicted theoretical histograms (red and blue curves), as calculated in two different ways (see below), in that the high-epsilon Hf values are missing. This leaves the false impression of no depleted component in the Hadean mantle and no memory of transient effects inherited from the original differentiation of the Earth. The red curves represent the mean and standard deviation of the three data sets calculated from the standard formulas, where potential problems are outliers and distribution tails. The blue curves represent the assessment of tails by least-square polynomial fit of the central part of the cumulated frequency plots. Both methods predict similar histograms, demonstrating that the assessment is robust. (For interpretation of the references to color in this figure legend, the reader is referred to the web version of this article.)

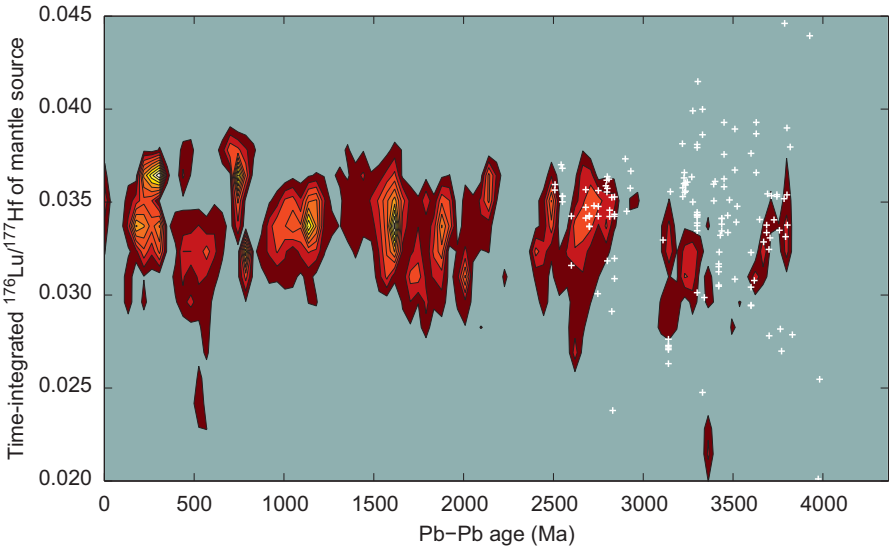

Fig. 8. Two-dimensional histogram of time-integrated $^{176}Lu/^{177}Hf$ of detrital and magmatic zircons (contours mark 10% intervals) as a function of their Pb-Pb age. The TTG whole-rock data of this study are superimposed as white crosses. (For interpretation of the references to color in this figure legend, the reader is referred to the web version of this article.)

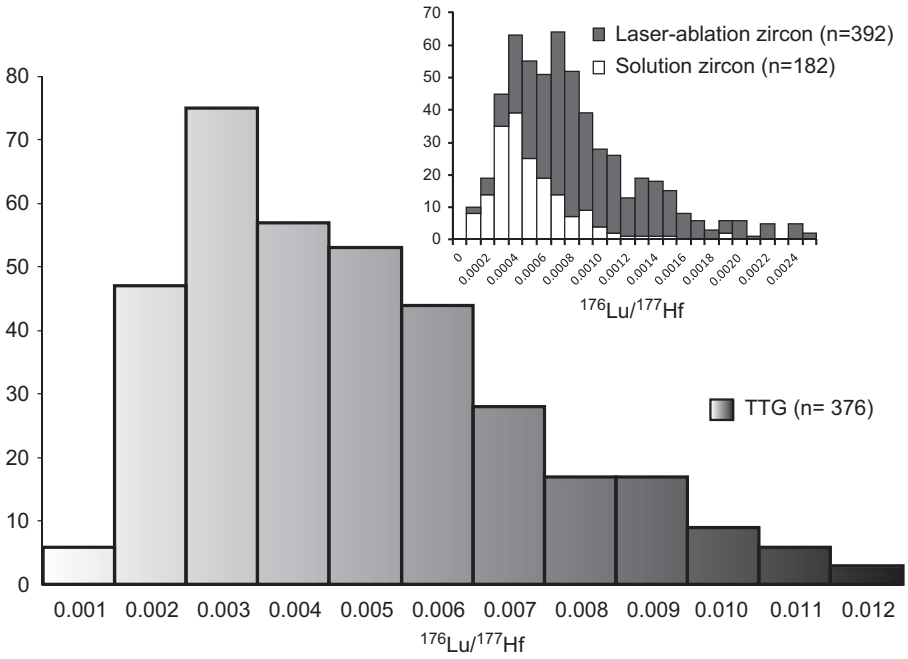

Fig. 9. Histogram of $^{176}Lu/^{177}Hf$ in TTGs from this study and the literature (references are listed in the Supplementary Material). The inset shows the $^{176}Lu/^{177}Hf$ distribution of zircons analyzed in this study. The gray bars represent laser-ablation $^{176}Lu/^{177}Hf$ measurements, while the white bars correspond to $^{176}Lu/^{177}Hf$ measured by solution chemistry. Note the broader range of the distribution for in-situ analyses compared to the single zircon dissolution technique, which overlaps with the low-Lu/Hf tail of the TTG whole-rock distribution.

isotopic variability early in Earth's history, as suggested by two independent isotopic records, is striking and can be interpreted in different ways. The time interval in question is conspicuously reminiscent of the half-life of ^{235}U, the major provider of radiogenic heat in the Hadean and which, for all geophysical intents and purposes, is an 'extinct' radioactivity. The decay of ^{235}U clearly is a forcing parameter for mantle convection. The termination of extreme mantle heterogeneity by the end of the Hadean also coincides with the end of the Late Heavy Bombardment of the inner Solar System. However, as long as it is not firmly established whether this event represents a spike or the final demise of accretion (Hartmann and Berman, 2000), its effect on terrestrial geodynamics cannot be properly understood. Alternatively, the large variability in the apparent Sm/Nd and Lu/Hf ratios of Early Archean samples may simply reflect a misconstrued primordial isotope composition of Nd and Hf in the Earth. The only strong statement that safely emerges from Fig. 8 is that the geochemically transient state of the Earth lasted for about 1 Gy (Albarède et al., 2000).

For ~4 Gy, extraction of continental crust does not, therefore, appear to have depleted the mantle source of the continental protolith (Fig. 8). Island arc rocks and, to an even greater extent, TTGs, are characterized by particularly low $^{176}Lu/^{177}Hf$ ratios ((Blichert-Toft and Albarède, 2008); Fig. 9) and strong depletions in Nb and Ta (Hoffmann et al., 2011; Kamber et al., 2002). Both types of magmas derive from mafic melts through a second-stage

process and do not represent melts extracted directly from the (ultramafic) mantle. In contrast, both mid-ocean ridge (MORB) and plateau basalts have $^{176}Lu/^{177}Hf$ ratios not very different from the chondritic value (0.033) (Blichert-Toft and Albarède, 1997, 2008; Bouvier et al., 2008), while the $^{176}Lu/^{177}Hf$ ratio of the modern depleted upper mantle (0.045 according to Salters and Stracke (2004) and 0.053 according to Workman and Hart (2005)) is estimated to be much higher. Trace element and isotopic evidence (Hofmann, 1997) further indicates that MORB originates in a mantle that went through multiple melt extraction events in the distant past. In addition, MORB extraction visibly is a continuous process, which conflicts with the episodic record of continental crust formation (Albarède, 1998a). A mantle resembling the modern upper (MORB) mantle therefore does not provide a suitable precursor for continents.

The continental protolith hence was extracted without noticeable geochemical fractionation from a part of the mantle whose incompatible element content remained geochemically unchanged for 4 Gy. We surmise that this undepleted source could be the deep mantle and that it remained largely undepleted simply because melting of the rising plume head transporting the deep mantle material upwards only occurred in the upper mantle. A rising diapir of deep mantle separating at rather shallow depth into a basaltic protolith (the plume head) and a refractory residue merging with the residual upper mantle constituted the first step. The equivalence of greenstone belts with oceanic plateaus, the episodic character of their extraction from the mantle, and the age correspondence with peaks of crustal growth are well established (Condie, 1995). Unfortunately, trace element geochemistry is of little help to support this suggestion: a compilation of 327 samples of oceanic plateaus (from 〈http://www.georoc.org/portal.php〉) gives a mean $^{176}Lu/^{177}Hf$ value of 0.027, but with a wide range of variation of 300%, which attests to the complexity of melting conditions in this environment. The second step takes place at subduction zones and involves the melting of thick oceanic plateaus to form the orogenic magmas that will accrete to pre-existing continental crust. The depleted residues could return to the upper mantle either through subduction (Condie, 1998; Rollinson, 1997) or by subsequent delamination of the underplated residues (Arndt and Goldstein, 1989; Plank, 2005; Rudnick and Fountain, 1995). The volume of deep-seated fertile mantle source available for continent formation therefore decreases with time but without experiencing major chemical changes. The strikingly constant Lu/Hf ratio of the continent protolith demonstrates a connection between crust-forming processes and deep-mantle dynamics. This interpretation is consistent with the prevalence of superplume events in crustal growth (Boher et al., 1992; Hawkesworth et al., 2010; Schubert and Sandwell, 1989; Stein and Goldstein, 1996), possibly triggered by mantle avalanches (Stein and Hofmann, 1994), and with the origin of some plateau basalts in ancient primitive mantle (Jackson and Carlson, 2011). There is, in contrast, no large-scale geochemical record of $\varepsilon_{Hf}(T_0) > 8$ and, hence, no record of direct upper mantle involvement in crustal growth prior to the late Proterozoic (Fig. 2). However incontrovertible the evidence of subduction-related magmatic activity on the present Earth, it seems that this process was not the primary cause of crustal growth during most of geologic history. Oceanic crust consumption at subduction zones and creation at ridge crests are two complementary surface expressions of mantle convection. The rate at which these processes proceed may vary, but there is no hint in the geological record that they repeatedly came to a full stop for protracted periods of time. Crustal growth is forcibly episodic, plate tectonics is not. In other words, the composition and the episodicity of crust formation is related to plume-driven processes, while the main mechanism able to transform oceanic plateaus into continental crust is subduction. In a two-stage process, the first stage is controlled by deep-mantle dynamics and the second stage is controlled by plate tectonics (subduction).

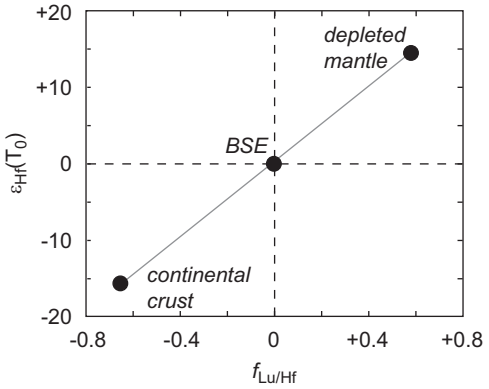

Fig. 10. Lu–Hf isochron diagram in normalized ε_{Hf} (T_0) and $f_{Lu/Hf}$ variables showing that the Bulk Silicate Earth (BSE=0,0), the depleted mantle, and continental crust form a good alignment, which supports that crust form from the BSE by leaving the depleted mantle as a residue. $f_{Lu/Hf}$ is defined as $[(^{176}Lu/^{177}Hf)_{sample}/(^{176}Lu/^{177}Hf)_{CHUR}]-1$, with $(^{176}Lu/^{177}Hf)_{CHUR}=0.0332$. The respective $^{176}Lu/^{177}Hf$ ratios of these reservoirs are those of Rudnick and Fountain (1995), Workman and Hart (2005), and Blichert-Toft and Albarède (1997). The mean present-day ε_{Hf} of the crust was taken from the average value of the Amazon bedload (Vervoort et al., 1999), while the value for the depleted mantle (+14) was taken from the maximum frequency of MORB samples in the GeoRoc database.

Defining the source of continental crust as the 'deep mantle' is nonetheless ambiguous as there is a need to assess how such an entity relates to the lower mantle defined by geophysics as the mantle underlying the 660 km seismic discontinuity. In the Lu–Hf isochron plot of Fig. 10, continental crust and the depleted mantle form an alignment with the bulk silicate Earth. The respective $^{176}Lu/^{177}Hf$ ratios of these reservoirs are those of Rudnick and Fountain (1995), Workman and Hart (2005), and Blichert-Toft and Albarède (1997). The mean ε_{Hf} (0) of the crust (−16) was taken from the average value of the Amazon bedload (Vervoort et al., 1999), for which U–Pb and Lu–Hf systematics in zircons show that it is overwhelmingly derived from the Precambrian catchment basin of Amazonia (Iizuka et al., 2010), while the value for the depleted mantle (+14) was taken from the maximum frequency of MORB samples in the GeoRoc database (〈http://www.georoc.org/portal.php〉). These values indicate that, upon crustal growth from a primitive mantle that leaves depleted MORB mantle as a residue, 46% of Hf fractionates into the crust. Using Hf concentrations of 0.28 ppm in the primitive mantle (McDonough and Sun, 1995), 3.7 ppm in the crust (Rudnick and Fountain, 1995), and 0.16 ppm in the depleted mantle (Workman and Hart, 2005), the proportion of the mantle depleted by crust formation is estimated to be 21%.

How does this interpretation differ from the decades-old paradigm of layered mantle convection and, in particular, how does subduction of lithospheric plates affect the composition of the deep mantle? Ancient fluxes of continental crust recycled into the mantle are poorly constrained. Scholl and von Huene (2009) acknowledged this limitation and assessed that the equivalent of the volume of modern crust may have been returned to the mantle over the last 3 Ga. The $^{40}K–^{40}Ar$ budget of crust and atmosphere formation clearly is incompatible with such a large volume. Coltice et al. (2000) showed that this volume is inconsistent with the $^{40}K–^{40}Ar$ budget of crust and atmosphere and used the amount of 'orphaned' ^{40}Ar in the atmosphere to bring the upper limit of crust recycled into the mantle over that period down to 25% of the present crust. One reason why fluxes of recycled continental crust are so low is that before sinking into the deep mantle, lithospheric plates are effectively stripped of their mobile elements, either because they are incompatible or because they are labile in the presence of fluids. Deep subduction

of barren plates (Albarède, 1998b) only negligibly changes the Lu/Hf ratio of the deep mantle, but dilutes incompatible element concentrations by up to a factor of two assuming present-day subduction rates and that all plates reach the lower mantle. If, by extrapolating the modern rate of plate subduction, it is assumed that a volume equivalent to that of the whole mantle has been processed through mid-ocean ridges, the proportion of the mantle depleted by crust formation should be raised from 21 to 40%. This range is to be compared with a mass proportion of 25% for the part of the mantle lying above the 660 km discontinuity, which seems to store plume material prior to eruption (Cao et al., 2011). If the deep mantle has a chondritic Lu/Hf ratio and a primordial Hf concentration, the modern upper mantle, therefore, is almost completely made up of residues of crust extraction. This cannot, however, have been the case for most of Earth's history, and hence largely accounts for, among other parameters that also play a role, the scarcity of ancient MORB-like magmas (Arndt, 2008).

The fertile mantle, which is the ultimate source of continental crust, therefore has receded downwards through geological time at the pace of crustal growth. Whichever proportion of U, Th, and K is presently hosted by the continental crust was, >3 Gy ago, still largely contained within the upper mantle and its activity substantially higher. Consequently, the temperature gradient in the upper mantle was significantly greater than its modern equivalent. In such a context, the predominant restriction of TTGs to crustal segments older than 1.8 Ga indicates that the geodynamics of the first ~ 3 Gy of Earth's history were controlled by hot partial melting of oceanic plateau basalts possibly in subduction-like environments (Condie et al., 2005), with both types of settings experiencing subsequent collisions, such as at Isua (Hiess et al., 2009), and the steady decantation of Mg-rich, buoyant depleted residues into the upper mantle.

6. Conclusions

This study addresses the long-standing and widely debated problem of the origin and evolution of the continental crust through Earth's history with special emphasis on the Hadean–Archean transition. We have revisited this question through a large new Lu–Hf isotope data set on a global collection of TTG rocks from almost every known craton, together with paired Hf (tracer) and Pb (age) isotopic measurements on single zircons from the same samples. The zircon work was undertaken with the goal of (i) demonstrating that the Hf isotopic compositions of zircons are representative of those of their host rock and, hence, can be used to make inferences about continental growth, and to (ii) either verify or determine the Pb–Pb ages of the samples. We also show that solution and laser-ablation Hf isotopic measurements are in good agreement. We use this data set, together with a large database of previously published Hf isotopic compositions on detrital and magmatic zircons, to show that the time-integrated Lu/Hf ratios recorded in TTGs and the global zircon database have remained essentially unchanged—and approximately similar to the chondritic ratio—over the past 4 Gy. We argue that the narrow range of near-chondritic Lu/Hf supports derivation of continental crust from primitive (chondritic) mantle instead of, as commonly assumed, the depleted upper mantle (MORB-source). We surmise that this primitive reservoir resides in the lower mantle, implying that continental crust is generated from a deep mantle source rather than the upper mantle. In this scenario, continental crust principally formed early on through partial melting at subduction zones of oceanic plateaus, which in turn formed by shallow melting of primitive mantle material brought from the lower mantle in upwelling plume heads. The depleted plume residues would remain in and merge with the upper mantle after crust extraction.

Acknowledgments

We are grateful to Geoscience Australia, Chris Carson, Olga Turkina, Valery Vetrin, Martin Van Kranendonk, Dave Champion, Minik Rosing, Thomas Naeraa, Jean-François Moyen, Mingguo Zhaï, Peng Peng, and Svetlana Lobach-Zhuchenko for generously providing most of the samples analyzed in this study. We further thank Philippe Telouk, Chantal Douchet, Emmanuelle Albalat, Florent Arnaud-Godet, Gilles Montagnac, Bertrand Van De Moortele, Jean-Louis Paquette, Jean-Marc Hénot, Denis Mangin, Marc Chaussidon, Wouter Bleeker, Mireille Besairie, Nicole Cates, Oleg Abramov, Craig Manning, Mark Harrison, Charles Knaack, Thomas Williams, Richard Gaschnig, and Jeff Vervoort for help with either technical or analytical matters or field work. JBT and FA acknowledge financial support from the French Programme National de Planétologie of the Institut National des Sciences de l'Univers and Centre National d'Etudes Spatiales, and from the French Agence Nationale de la Recherche (grants BEGDy – Birth and Evolution of Terrestrial GeoDynamics and M&Ms – Mantle Melting – Measurements, Models, Mechanisms), while SJM acknowledges financial support from the NASA Exobiology Program (grant Exploring the Hadean Earth) and NASA Lunar Science Institute Program (Center for Lunar Origin and Evolution), the National Geographic Society, University of Colorado and the J. William Fulbright Foundation. We thank Matthew Jackson for inspiring discussion and Klaus Mezger and an anonymous reviewer for their helpful comments.

Appendix A. Supplementary material

Supplementary data associated with this article can be found in the online version at http://dx.doi.org/10.1016/j.epsl.2012.05.029.

References

Abouchami, W., Boher, M., Michard, A., Albarède, F., 1990. A major 2.1 Ga event of mafic magmatism in West Africa—an early stage of crustal accretion. J. Geophys. Res. 95, 17605–17629.
Albarède, F., 1998a. The growth of continental crust. Tectonophysics 296, 1–14.
Albarède, F., 1998b. Time-dependent models of U–Th–He and K–Ar evolution and the layering of mantle convection. Chem. Geol. 145, 413–429.
Albarède, F., Blichert-Toft, J., Vervoort, J.D., Gleason, J.D., Rosing, M., 2000. Hf–Nd isotope evidence for a transient dynamic regime in the early terrestrial mantle. Nature 404, 488–490.
Albarède, F., Brouxel, M., 1987. The Sm/Nd secular evolution of the continental crust and the depleted mantle. Earth Planet. Sci. Lett. 82, 25–35.
Albarède, F., Telouk, P., Blichert-Toft, J., Boyet, M., Agranier, A., Nelson, B., 2004. Precise and accurate isotopic measurements using multiple-collector ICPMS. Geochim. Cosmochim. Acta 68, 2725–2744.
Arndt, N.T., 2008. Komatiites. Cambridge University Press.
Arndt, N.T., Goldstein, S.L., 1989. An open boundary between lower continental crust and mantle: its role in crust formation and crustal recycling. Tectonophysics 161, 201–212.
Bahlburg, H., Vervoort, J.D., DuFrane, S.A., Carlotto, V., Reimann, C., Cárdenas, J., 2011. The U–Pb and Hf isotope evidence of detrital zircons of the Ordovician Ollantaytambo Formation, southern Peru, and the Ordovician provenance and paleogeography of southern Peru and northern Bolivia. J. S. Am. Earth Sci. 32, 196–209.
Bennett, V.C., Brandon, A.D., Nutman, A.P., 2007. Coupled ^{142}Nd–^{143}Nd isotopic evidence for Hadean mantle dynamics. Science 318, 1907–1910.
Bennett, V.C., Nutman, A.P., McCulloch, M.T., 1993. Nd isotopic evidence for transient, highly depleted mantle reservoirs in the early history of the Earth. Earth Planet. Sci. Lett. 119, 299–317.
Blichert-Toft, J., 2001. On the Lu–Hf isotope geochemistry of silicate rocks. Geostandards Newsl. 25, 41–56.
Blichert-Toft, J., Albarède, F., 1997. The Lu–Hf isotope geochemistry of chondrites and the evolution of the mantle–crust system. Earth Planet. Sci. Lett. 148, 243–258.

Blichert-Toft, J., Albarède, F., 2008. Hafnium isotopes in Jack Hills zircons and the formation of the Hadean crust. Earth Planet. Sci. Lett. 265, 686–702.
Blichert-Toft, J., Boyet, M., Télouk, P., Albarède, F., 2002. ^{147}Sm–^{143}Nd and ^{176}Lu–^{176}Hf in eucrites and the differentiation of the HED parent body. Earth Planet. Sci. Lett. 204, 167–181.
Blichert-Toft, J., Chauvel, C., Albarède, F., 1997. Separation of Hf and Lu for high-precision isotope analysis of rock samples by magnetic sector-multiple collector ICP-MS. Contrib. Mineral. Petrol. 127, 248–260.
Blichert-Toft, J., Puchtel, I.S., 2010. Depleted mantle sources through time: evidence from Lu–Hf and Sm–Nd isotope systematics of Archean komatiites. Earth Planet. Sci. Lett. 297, 598–606.
Boher, M., Abouchami, W., Michard, A., Albarède, F., Arndt, N.T., 1992. Crustal growth in West-Africa at 2.1 Ga. J. Geophys. Res. 97, 345–369.
Bouvier, A., Vervoort, J.D., Patchett, P.J., 2008. The Lu–Hf and Sm–Nd isotopic composition of CHUR: constraints from unequilibrated chondrites and implications for the bulk composition of terrestrial planets. Earth Planet. Sci. Lett. 273, 48–57.
Bowring, S.A., Williams, I.S., Compston, W., 1989. 3.96 Ga gneisses from the Slave Province, Northwest-Territories, Canada. Geology 17, 971–975.
Cao, Q., van der Hilst, R.D., de Hoop, M.V., Shim, S.H., 2011. Seismic imaging of transition zone discontinuities suggests hot mantle west of Hawaii. Nature 332, 1068–1071.
Carson, C.J., Ague, J.J., Grove, M., Coath, C.D., Harrison, T.M., 2002. U–Pb isotopic behaviour of zircon during upper-amphibolite facies fluid infiltration in the Napier Complex, east Antarctica. Earth Planet. Sci. Lett. 199, 287–310.
Cherniak, D.J., Hanchar, J.M., Watson, E.B., 1997a. Diffusion of tetravalent cations in zircon. Contrib. Mineral. Petrol. 127, 383–390.
Cherniak, D.J., Hanchar, J.M., Watson, E.B., 1997b. Rare-earth diffusion in zircon. Chem. Geol. 134, 289–301.
Coltice, N., Albarède, F., Gillet, P., 2000. ^{40}K–^{40}Ar constraints on recycling continental crust into the mantle. Science 288, 845–847.
Condie, K.C., 1995. Episodic ages of greenstones: a key to mantle dynamics? Geophys. Res. Lett. 22, 2215–2218.
Condie, K.C., 1998. Episodic continental growth and supercontinents: a mantle avalanche connection? Earth Planet. Sci. Lett. 163, 97–108.
Condie, K.C., Belousova, E., Griffin, W.L., Sircombe, K.N., 2009a. Granitoid events in space and time: constraints from igneous and detrital zircon age spectra. Gondwana Res. 15, 228–242.
Condie, K.C., Beyer, E., Belousova, E., Griffin, W.L., O'Reilly, S.Y., 2005. U–Pb isotopic ages and Hf isotopic composition of single zircons: the search for juvenile Precambrian continental crust. Precambrian Res. 139, 42–100.
Corfu, F., 2000. Extraction of Pb with artificially too-old ages during stepwise dissolution experiments on Archean zircon. Lithos 53, 279–291.
Das, A., Davis, D.W., 2010. Response of Precambrian zircon to the chemical abrasion (CA-TIMS) method and implications for improvement of age determinations. Geochim. Cosmochim. Acta 74, 5333–5348.
Davis, D.W., Amelin, Y., Nowell, G.M., Parrish, R.R., 2005. Hf isotopes in zircon from the western Superior province, Canada: implications for Archean crustal development and evolution of the depleted mantle reservoir. Precambrian Res. 140, 132–156.
DePaolo, D.J., 1980. Crustal growth and mantle evolution: inferences from models of element transport and Nd and Sr isotopes. Geochim. Cosmochim. Acta 44, 1185–1196.
DePaolo, D.J., 1981. A neodymium and strontium isotopic study of the Mesozoic calc-alkaline granitic batholiths of the Sierra Nevada and Peninsular Ranges, California. J. Geophys. Res. 86, 10470–10488.
Dickinson, W.R., Gehrels, G.E., 2003. U–Pb ages of detrital zircons from Permian and Jurassic eolian sandstones of the Colorado Plateau, USA: paleogeographic implications. Sediment. Geol. 163, 29–66.
Drummond, M.S., Defant, M.J., 1990. A model for trondhjemite–tonalite–dacite genesis and crustal growth via slab melting: Archean to modern comparisons. J. Geophys. Res. 95, 503–521.
Eisele, J., Abouchami, W., Galer, S.J.G., Hofmann, A.W., 2003. The 320 kyr Pb isotope evolution of Mauna Kea lavas recorded in the HSDP-2 drill core. Geochem. Geophys. Geosyst. 4, 1–32.
Gaschnig, R.M., Vervoort, J.D., Lewis, R.S., Tikoff, B., 2011. Isotopic evolution of the Idaho Batholith and Challis Intrusive Province, Northern US Cordillera. J. Petrol. 52, 2397–2429.
Gastil, G., 1960. The distribution of mineral dates in space and time. Am. J. Sci. 258, 1–35.
Gurnis, M., Davies, G.J., 1986. Apparent episodic crustal growth arising from a smoothly evolving mantle. Geology 14, 396–399.
Harrison, T.M., Blichert-Toft, J., Müller, W., Albarede, F., Holden, P., Mojzsis, S.J., 2005. Heterogeneous Hadean hafnium: evidence of continental crust at 4.4 to 4.5 Ga. Science 310, 1947–1950.
Harrison, T.M., Schmitt, A.K., McCulloch, M.T., Lovera, O.M., 2008. Early ($\geq$4.5 Ga) formation of terrestrial crust: Lu-Hf, δ^{18}O, and Ti thermometry results for Hadean zircons. Earth Planet. Sci. Lett. 268, 476–486.
Hartmann, W.K., Berman, D.C., 2000. Elysium Planitia lava flows: crater counts chronology and geological implications. J. Geophys. Res. 105, 15011–15025.
Hawkesworth, C.J., Dhuime, B., Cadwood, P.A., Kemp, A.I.S., Storey, C.D., 2010. The generation and evolution of the continental crust. J. Geol. Soc. London 167, 229–248.
Hiess, J., Bennett, V.C., Nutman, A.P., Williams, I.S., 2009. In situ U–Pb, O and Hf isotopic compositions of zircon and olivine from Eoarchaean rocks, West Greenland: new insights to making old crust. Geochim. Cosmochim. Acta 73, 4489–4516.
Hoffman, P.F., 1988. United plates of America, the birth of a craton: early Proterozoic assembly and growth of Laurentia. Ann. Rev. Earth Planet. Sci. 16, 543–603.
Hoffmann, J.E., Münker, C., Næraa, T., Rosing, M.T., Herwartz, D., Garbe-Schönberg, D., Svahnberg, H., 2011. Mechanisms of Archean crust formation inferred from high-precision HFSE systematics in TTGs. Geochim. Cosmochim. Acta 75, 4157–4178.
Hofmann, A.W., 1997. Mantle geochemistry: the message from oceanic volcanism. Nature 385, 219–229.
Hoskin, P.W.O., Schaltegger, U., 2003. The composition of zircon and igneous and metamorphic petrogenesis, Zircon. Mineralogical Society of America and The Geochemical Society (pp. 27–62).
Iizuka, T., Komiya, T., Rino, S., Maruyama, S., Hirata, T., 2010. Detrital zircon evidence for Hf isotopic evolution of granitoid crust and continental growth. Geochim. Cosmochim. Acta 74, 2450–2472.
Jackson, M.G., Carlson, R.W., 2011. An ancient recipe for flood-basalt genesis. Nature 476, 316–319.
Jacobsen, S.B., Wasserburg, G.J., 1979. The mean age of mantle and crustal reservoirs. J. Geophys. Res. 84, 7411–7427.
Kamber, B.S., Ewart, A., Collerson, K.D., Bruce, M.C., McDonald, G.D., 2002. Fluid-mobile trace element constraints on the role of slab melting and implications for Archaean crustal growth models. Contrib. Mineral. Petrol. 144, 38–56.
Kelemen, P.B., 1995. Genesis of high Mg# andesites and the continental crust. Contrib. Mineral. Petrol. 120, 1–19.
Kemp, A.I.S., Hawkesworth, C.J., Foster, G.L., Paterson, B.A., Woodhead, J.D., Hergt, J.M., Gray, C.M., Whitehouse, M.J., 2007. Magmatic and crustal differentiation history of granitic rocks from Hf–O isotopes in zircon. Science 315, 980–983.
Kemp, A.I.S., Hawkesworth, C.J., Paterson, B.A., Kinny, P.D., 2006. Episodic growth of the Gondwana supercontinent from hafnium and oxygen isotopes in zircon. Nature 439, 580–583.
Kemp, A.I.S., Wilde, S.A., Hawkesworth, C.J., Coath, C.D., Nemchin, A., Pidgeon, R.T., Vervoort, J.D., DuFrane, S.A., 2010. Hadean crustal evolution revisited: new constraints from Pb–Hf isotope systematics of the Jack Hills zircons. Earth Planet. Sci. Lett. 296, 45–56.
Kistler, R.W., Wooden, J.L., Morton, D.M., 2003. Isotopes and Ages in the Northern Peninsular Ranges Batholith, Southern California. USGS Open-File Report 03-489. pp. 45.
Krogh, T.E., 1982. Improved accuracy of U–Pb zircon ages by the creation of more concordant systems using an air abrasion technique. Geochim. Cosmochim. Acta 46, 637–649.
Lenting, C., Geisler, T., Gerdes, A., Kooijman, E., Scherer, E.E., Zeh, A., 2010. The behavior of the Hf isotope system in radiation-damaged zircon during experimental hydrothermal alteration. Am. Min. 95, 1343–1348.
Martin, H., 1993. The mechanisms of petrogenesis of the Archaean continental crust—comparison with modern processes. Lithos 30, 373–388.
Mattinson, J., 2005. Zircon U–Pb chemical abrasion ("CA-TIMS") method: combined annealing and multi-step partial dissolution analysis for improved precision and accuracy of zircon ages. Chem. Geol. 220, 47–66.
McDonough, W.F., Sun, S.S., 1995. The composition of the Earth. Chem. Geol. 120, 223–253.
Nyquist, L.E., Shih, C.-Y., 1992. The isotopic record of lunar volcanism. Geochim. Cosmochim. Acta 56, 2213–2234.
Paces, J.B., Miller, J.D., 1993. Precise U–Pb ages of Duluth Complex and related mafic intrusions, northeastern Minnesota geochronological insights to physical, petrogenetic, paleomagnetic, and tectonomagmatic processes associated with the 1.1 Ga midcontinent rift system. J. Geophys. Res. 98, 13997–14013.
Parrish, R.R., 1987. An improved micro-capsule for zircon dissolution in U–Pb geochronology. Chem. Geol. 66, 99–102.
Patchett, P.J., Kouvo, O., Hedge, C.E., Tatsumoto, M., 1981. Evolution of continental crust and mantle heterogeneity: evidence from Hf isotopes. Contrib. Mineral. Petrol. 78, 279–297.
Patchett, P.J., Todt, W., Gorbatschev, R., 1987. Origin of continental crust of 1.9–1.7 Ga age: Nd isotopes in the Svecofennian orogenic terrains of Sweden. Precambrian Res. 35, 145–160.
Plank, T., 2005. Constraints from thorium/lanthanum on sediment recycling at subduction zones and the evolution of the continents. J. Petrol. 46, 921–944.
Rollinson, H., 1997. Eclogite xenoliths in west African kimberlites as residues from Archaean granitoid crust formation. Nature 389, 173–176.
Rudnick, R.L., Fountain, D.M., 1995. Nature and composition of the continental crust: a lower crustal perspective. Rev. Geophys. 33, 267–309.
Salters, V.J.M., Stracke, A., 2004. Composition of the depleted mantle. Geochem. Geophys. Geosyst. 5, Q05004.
Scherer, E., Münker, C., Mezger, K., 2001. Calibration of the lutetium–hafnium clock. Science 293, 683–687.
Scholl, D.W., von Huene, R., 2009. Implications of estimated magmatic additions and recycling losses at the subduction zones of accretionary (non-collisional) and collisional (suturing) orogens. Geol. Soc. London Spec. Publ. 318, 105–125.
Schubert, G., Sandwell, D., 1989. Crustal volumes of the continents and of oceanic and continental submarine plateaus. Earth Planet. Sci. Lett. 92, 234–246.
Shirey, S.B., Hanson, G.N., 1986. Mantle heterogeneity and crustal recycling in Archean granite-greenstone belts: evidence from Nd isotopes and trace elements in the Rainy Lake area, Superior Province, Ontario, Canada. Geochim. Cosmochim. Acta 50, 2631–2651.
Söderlund, U., Patchett, P.J., Vervoort, J.D., Isachsen, C.E., 2004. The ^{176}Lu decay constant determined by Lu–Hf and U–Pb isotope systematics of Precambrian mafic intrusions. Earth Planet. Sci. Lett. 219, 311–324.

Stacey, J.S., Kramers, J.D., 1975. Approximation of terrestrial lead isotope evolution by a two-stage model. Earth Planet. Sci. Lett. 26, 207–221.
Stein, M., Goldstein, S.L., 1996. From plume head to continental lithosphere in the Arabian-Nubian shield. Nature 382, 773–778.
Stein, M., Hofmann, A.W., 1994. Mantle plumes and episodic crustal growth. Nature 372, 63–68.
Taylor, H.P., Silver, L.T., 1978. Oxygen Isotope Relationships in Plutonic Igneous Rocks of the Peninsular Ranges Batholith, Southern and Baja California. USGS Open-File Report 78-701. pp. 423–436.
Utsunomiya, S., Palenik, C.S., Valley, J.W., Cavosie, A.J., Wilde, S.A., Ewing, R.C., 2004. Nanoscale occurrence of Pb in an Archean zircon. Geochim. Cosmochim. Acta 68, 4679–4686.
Vervoort, J.D., Blichert-Toft, J., 1999. Evolution of the depleted mantle: Hf isotope evidence from juvenile rocks through time. Geochim. Cosmochim. Acta 63, 533–556.
Vervoort, J.D., Patchett, P.J., Blichert-Toft, J., Albarède, F., 1999. Relationships between Lu–Hf and Sm–Nd isotopic systems in the global sedimentary system. Earth Planet. Sci. Lett. 168, 79–99.
Workman, R.K., Hart, S.R., 2005. Major and trace element composition of the depleted MORB mantle (DMM). Earth Planet. Sci. Lett. 231, 53–72.
Zeh, A., Gerdes, A., Klemd, R., Barton, J.M., 2007. Archaean to Proterozoic Crustal evolution in the Central Zone of the Limpopo Belt (South Africa-Botswana): constraints from combined U–Pb and Lu–Hf isotope analyses of zircon. J. Petrol. 48, 1605–1639.